

Doppler cloak restores invisibility to objects in relativistic motion

Davide Ramaccia,^{1,*} Dimitrios L. Sounas,² Andrea Alù,² Alessandro Toscano,¹ and Filiberto Bilotti¹

¹*Department of Engineering, “Roma Tre” University, Via Vito Volterra 62, 00146 Rome, Italy*

²*Department of Electrical and Computer Engineering, The University of Texas at Austin, Austin, Texas 78712, USA*

(Received 7 January 2016; revised manuscript received 28 November 2016; published 6 February 2017)

Although cloaks are effective at suppressing the observability of static objects, they can be defeated when in motion. Here we discuss a general technique to cloak the motion of objects from static observers, based on compensating the Doppler shift associated with their motion with frequency conversion sustained by a spatiotemporally modulated cover. The concept is theoretically and numerically demonstrated in a system composed of a planar reflector covered by a spatiotemporally modulated slab. It is shown that, for properly selected modulation frequency, the composite system can appear to an external observer as stationary, even though it is actually moving. This concept may pave the way to the minimization of clutter produced by moving objects as well as to new directions in the science of cloaking.

DOI: [10.1103/PhysRevB.95.075113](https://doi.org/10.1103/PhysRevB.95.075113)

Invisibility cloaks, which can make objects undetectable to an external observer based, for instance, on transformation electromagnetics [1,2] and scattering cancellation [3,4], have attracted a large research interest in the past decade [5]. Both techniques, as well as other available approaches based on passive metamaterials, are subject to fundamental limitations that restrict the overall bandwidth over which invisibility can be achieved [6]. It has recently been discussed how similar fundamental issues arise when considering cloaking of moving objects, even under illumination with narrow-band signals [7]. In particular, the Doppler effect that arises in moving systems [8] may shift the frequency of the impinging wave outside the cloaking bandwidth, thus, eliminating or seriously affecting the cloaking effect. A possible way to overcome this problem is to design the cloak to operate at the Doppler-shifted frequency instead of the frequency of the impinging wave. However, such an approach can restore the cloaking effect only for one propagation direction and for a specific velocity, whereas the object remains detectable in other scenarios [7].

Here, we explore the general problem of restoring the cloaking effect of a moving object for any incidence direction. Inspired by the mantle cloaking technique, based on which a properly designed metamaterial cover is able to cancel the total scattering from a scatterer [4,9], we explore covering a moving object with a metamaterial that is able to compensate for the Doppler shift associated with the motion by generating a frequency shift opposite to the one of the Doppler effect. The basic operation of such a cloak is illustrated in Fig. 1. An object moving with velocity v_0 with respect to a static source creates a frequency shift δf for the scattered field as illustrated in Fig. 1(a). The Doppler cloak is designed to compensate for such a shift, creating a frequency shift $-\delta f$ as illustrated in Fig. 1(b). Such a system is necessarily active since all passive systems exhibit an identical Doppler effect when moving with the same velocity. Then, by covering the moving object with the Doppler cloak as in Fig. 1(c), we may be able to achieve

a zero-frequency shift from the composite system, making the object look at rest, despite the fact that it is actually moving.

In this paper, we demonstrate the Doppler cloak concept for the basic scenario of backscattering from a moving reflector. In order to achieve a frequency shift that cancels the Doppler effect, the reflector is covered by a *momentum-biased metamaterial*, whose artificial permittivity function is modulated in space and time. Such a metamaterial exhibits frequency mixing properties, which have recently been explored for the realization of nonreciprocal devices [10–17]. As shown in the following, this nonreciprocal effect is also important for the operation of the proposed Doppler cloak.

In addition to constituting a relevant step towards full cloaking of moving objects, which can now appear at rest and can therefore be cloaked with conventional techniques, the proposed solution opens interesting possibilities to eliminate the Doppler interference caused by moving objects, such as wind and tidal power plant installations, on the operation of velocity radars, such as land Doppler radars. Although the Doppler cancellation concept is demonstrated here for the simple case of a linearly moving mirror, there is no fundamental limitation for extending its application to objects of more complex shapes and different motions as discussed in the following. The proposed technique is different from conventional radar countermeasures, which typically are based on signal jamming [18]. Our approach also provides an exciting demonstration of the large opportunities offered by active cloaks for overcoming fundamental limitations of their passive counterparts as was shown recently in the context of non-Foster [19], externally driven [20], and parity-time symmetric cloaks [21].

A way to achieve the required frequency shift is based on spatiotemporal modulation of the material constituting the Doppler cloak. In particular, we choose to modulate the properties of a dielectric slab according to the traveling-wave profile $\varepsilon_r(z, t) = \varepsilon_{r_0} + \delta\varepsilon \cos(\omega_m t + k_m z)$, where ε_{r_0} is the intrinsic (unmodulated) permittivity, $\delta\varepsilon$ is the modulation depth, ω_m is the modulation frequency, and k_m is the modulation wave number. Figure 2(b) presents two snapshots of this modulation profile, demonstrating its traveling-wave character towards the $-z$ direction. A possible implementation of an artificial material whose permittivity is locally and dynamically modified

* Author to whom correspondence should be addressed:
davide.ramaccia@uniroma3.it

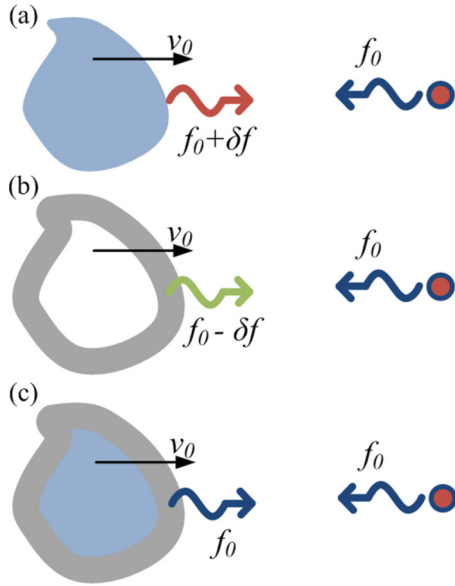


FIG. 1. (a) Conventional Doppler effect for an object moving towards a stationary source with velocity v_0 . The frequency of the reflected signal is increased by a quantity δf related to the velocity v_0 of the object. (b) A Doppler cloak is capable of compensating the Doppler shift δf of the moving object. (c) Doppler-cloaked object induces zero-frequency shift to an impinging wave, despite the fact that it is moving.

by an external electric field has recently been proposed in Ref. [22]. The modulated slab can induce a frequency shift $\pm\omega_m$ for waves propagating through it if the modulation signal provides phase matching between the incident wave and another wave in the slab [23]. The conditions that describe such phase matching read $\omega_1 - \omega_0 = \pm\omega_m$ and $k_1 - k_0 = \mp k_m$, where ω_0 and k_0 are the frequency and wave number of the incident wave and ω_1 and k_1 are the corresponding parameters for the phase-matched wave. Such a phase-matching process is the result of intraband transitions, and it is explained visually in Fig. 2(c) for a slab with frequency-independent phase velocity $v_{ph} = c/\sqrt{\epsilon_{r0}}$ (linear dispersion $\omega/k = \pm v_{ph}$) and a modulation signal with $\omega_m/k_m = v_{ph}$, i.e., the same phase velocity as the propagating waves in the slab. In such a scenario, the incident wave is phase matched to two modes, resulting in two output frequencies $\omega_{1+} = \omega + \omega_m$ and $\omega_{1-} = \omega - \omega_m$. Phase matching is satisfied only for

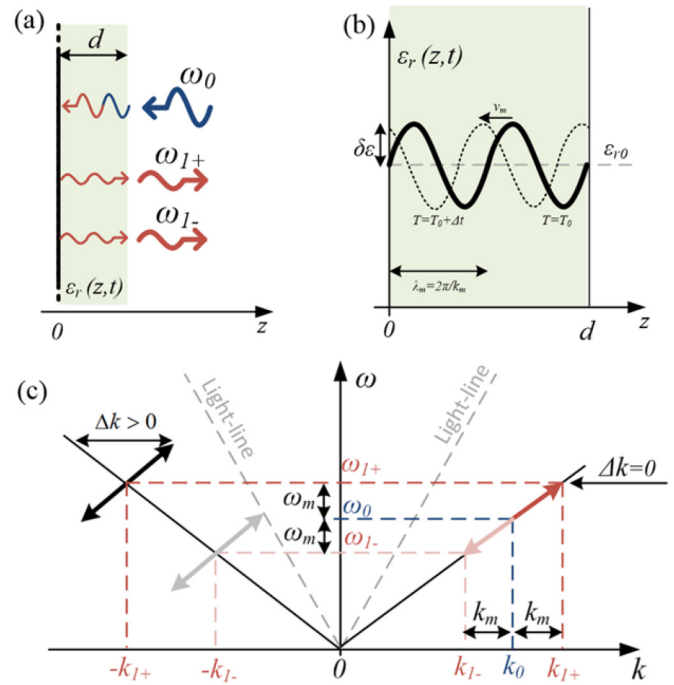


FIG. 2. (a) Planar reflector at rest loaded with a spatiotemporally modulated metamaterial cover. The incident signal at frequency ω_0 is converted into two signals at frequencies ω_{1+} and ω_{1-} due to the interaction with the momentum-biased metamaterial. (b) The modulation profile at two sequential time steps. (c) Dispersion diagram for the wave propagation through the metamaterial. The arrows indicate the frequency and wave-vector shifts induced by the modulation.

waves propagating in the $-z$ direction, implying that the aforementioned frequency conversion is observed only for this propagation direction not for the opposite one. This is a clear demonstration of nonreciprocal response, and it has recently inspired the design of nonreciprocal devices based on spatiotemporal modulation [10–17].

The frequency-conversion properties of the spatiotemporally modulated slab can be quantified through a coupled-mode analysis [24]. Considering that $\omega_m/k_m = \omega_0/k_0 = \omega_{1\pm}/k_{1\pm} = v_{ph}$ due to the common phase velocity for all the waves propagating in the slab, including the modulation signal, the coupled-mode equations can be derived as

$$\begin{aligned} \frac{d}{dz} A_0(z) &= \frac{1}{2jk_0} \left[\left(-\frac{\omega_0^2}{c^2} \epsilon_{r0} + k_0^2 \right) A_0(z) - \frac{1}{2} \frac{\omega_0^2}{c^2} \delta\epsilon A_{1-}(z) - \frac{1}{2} \frac{\omega_0^2}{c^2} \delta\epsilon A_{1+}(z) \right], \\ \frac{d}{dz} A_{1-}(z) &= \frac{1}{2jk_{1-}} \left[-\frac{1}{2} \frac{\omega_{1-}^2}{c^2} \delta\epsilon A_0(z) + \left(-\frac{\omega_{1-}^2}{c^2} \epsilon_{r0} + k_{1-}^2 \right) A_{1-}(z) \right], \\ \frac{d}{dz} A_{1+}(z) &= \frac{1}{2jk_{1+}} \left[-\frac{1}{2} \frac{\omega_{1+}^2}{c^2} \delta\epsilon A_0(z) + \left(-\frac{\omega_{1+}^2}{c^2} \epsilon_{r0} + k_{1+}^2 \right) A_{1+}(z) \right], \end{aligned} \quad (1)$$

where A_0 , A_{1-} , and A_{1+} are the complex amplitudes of the waves with frequencies ω_0 , ω_{1-} , and ω_{1+} , respectively. Requiring that at the slab input $z = 0$ the energy is maximum for the mode (ω_0, k_0) and zero for the modes $(\omega_{1\pm}, k_{1\pm})$, we obtain the solution,

$$A_0(z) = E_0 \cos(k_C z), \quad A_{1-}(z) = \frac{E_0}{\sqrt{2}} \frac{k_{1-}}{k_0} \sin(k_C z), \quad A_{1+}(z) = \frac{E_0}{\sqrt{2}} \frac{k_{1+}}{k_0} \sin(k_C z), \quad (2)$$

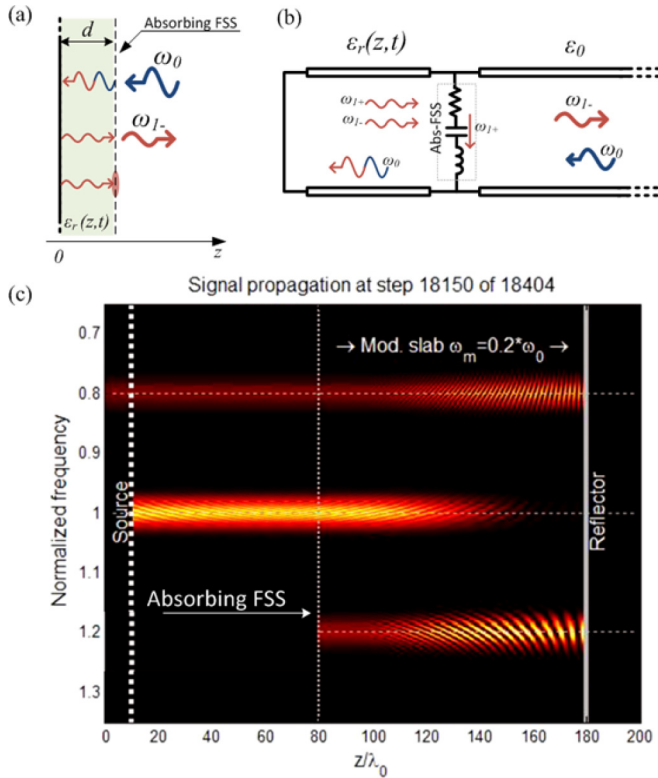


FIG. 3. (a) Planar reflector at rest covered with a spatiotemporally modulated metamaterial slab and an absorbing metasurface. The metasurface absorbs the signal at frequency ω_{1+} . (b) Equivalent transmission-line model of the structure in panel (a). (c) Time-domain response of the metamaterial-covered reflector in panel (a). Results are obtained through finite-difference time-domain (FDTD) simulations for $\kappa = 7.07 \times 10^{-3}$ and $\omega_m = 0.2\omega_0$.

where $k_C = \kappa k_0 / (2\sqrt{2})$ is the coupling wavelength and $\kappa = \delta\varepsilon / \varepsilon_{r0}$ is the relative amplitude of the modulation. It is obvious from Eq. (2) that the incident signal is converted totally into signals at frequencies $\omega_{1\pm}$ after a propagation length $\ell_c = \pi / 2k_C$, referred to as the coherence length [25]. In

order to achieve total conversion of the incident signal at the end of the slab, its thickness d must be equal to ℓ_c . Equation (1) can also be used to derive the response of the slab when it is excited from its left-hand side with a wave propagating along the $+z$ direction. In such a case, phase matching is not possible as seen in Fig. 2(c), and the frequency conversion of the incident signal is very weak. In fact, for the practically important case of propagation length equal to the coherence length, the frequency conversion is identically zero [25]. It is worth mentioning that the intraband energy transfer enabled by the modulated cover takes place as long as the propagation direction of the modulated permittivity profile is parallel to the propagation direction of the incident field. However, for moderate misalignments, the intraband transition still occurs with high efficiency, but, in general, in the case of oblique incidence, the modulation profile needs to be controlled dynamically in order to be aligned to the incidence propagation direction (refer to the Supplemental Material for the discussion on the angular and frequency bandwidths of the Doppler cloak [26]). Even in the case of finite-sized objects the intraband energy transfer can be induced efficiently by properly selecting the modulation profile of the linear momentum-biased metamaterial.

Consider now the case in which the spatiotemporally modulated slab analyzed above is placed in front of a planar metallic mirror that reflects all incident electromagnetic energy as illustrated in Fig. 2(a). We highlight that, in the case of a mirror with finite reflectivity, due to absorption or transmission, the amount of energy reflected back by the reflector will be less than unity. However, this will not affect the operation of the spatiotemporal modulated cover, which operates in the same way regardless of the mirror characteristics. The mirror initially is assumed at rest. An impinging wave from the right-hand side of this system propagates through the slab along the $-z$ direction, then it is reflected by the mirror and exits the system after propagating again through the slab in the $+z$ direction. Due to the spatiotemporal modulation of the slab, the incident wave experiences full frequency conversion before reaching the mirror as it propagates along the $-z$ direction in the slab. At the same time, the nonreciprocal

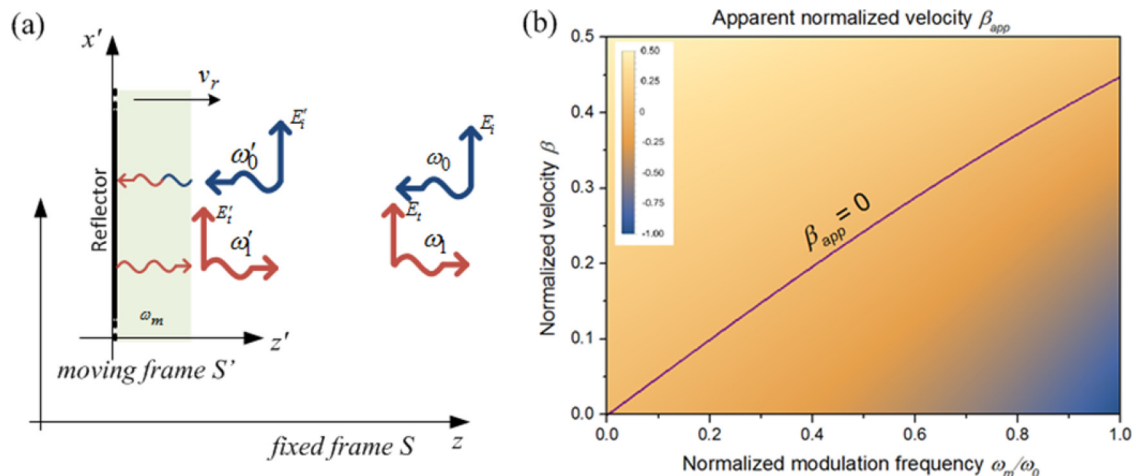


FIG. 4. (a) Metamaterial-covered reflector moving in the $+z$ direction at velocity v_r . Primed and unprimed quantities refer to the moving and stationary frames, respectively. (b) Apparent normalized velocity detected from an external observer as a function of the normalized actual velocity β and the modulated frequency ω_m / ω_0 . The solid curve indicates the points for which the apparent velocity vanishes, i.e., $\beta_{app} = 0$.

properties of the spatiotemporally modulated slab prevent the reflected signal from the mirror to be converted back to the original frequency. As a result, regardless of the actual moving direction of the traveling-wave profile of permittivity [27], the reflected wave from the composite structure is a linear combination of two frequency components $\omega_{1\pm}$ shifted from ω_0 by ω_m . Such a reflected field will be perceived by an external observer as the one created by a pair of moving scatterers with velocities $v_{\pm} = c/(1 \pm 2\omega_0/\omega_m)$, corresponding to Doppler shifts $\Delta\omega_{\pm} = \omega_{1\pm} - \omega_0$. Notice that one of these effective scatterers moves towards the source with velocity $v_+ = c/(1 + 2\omega_0/\omega_m)$, whereas the other one moves in the opposite direction with velocity $|v_-| = c/(2\omega_0/\omega_m - 1)$. It is evident that the former (latter) effect can be used to compensate for the Doppler shift resulting from the composite system moving away (towards) the source. For a given motion direction, only one of the effective Doppler shifts is useful to compensate the actual Doppler effect, whereas the other one is parasitic.

There are different ways to cancel this parasitic effect. For example, a simple solution may be to add a metasurface that absorbs the parasitic frequency and transmits the other signals in front of the spatiotemporally modulated metasurface as in Fig. 3(a). Such an approach leads to reduced efficiency (50% maximum). Another more efficient approach may be based on implementing a slab with frequency-dependent phase velocity (nonlinear $\omega - k$ dispersion) so that the phase-matching condition is satisfied only for one of the frequencies $\omega_{1\pm}$. For example, for a system moving away from the source, an effective plasma slab, consisting of an array of parallel plate waveguides, may be considered with an effective plasma frequency larger than ω_{1-} so that the photonic transition to this frequency, i.e., to the Doppler-shifted frequency for an object moving away from the source, would not be possible. However, due to the nonlinear dispersion of the material supporting the permittivity modulation, the operating band is reduced due to the high phase mismatch that may occur between the original mode and the induced one. More details about such a system are provided in Ref. [28]. Here, for simplicity of analysis, we follow the absorbing-metasurface approach described above for a system moving towards the source. In such a case, the metasurface is designed to absorb ω_{1+} and transmit ω_0 and ω_{1-} . The response in the absence of motion has been obtained through a FDTD numerical simulation of the transmission-line equivalent in Fig. 3(b), and it is presented in Fig. 3(c). The numerical results are in perfect agreement with the aforementioned theoretical description.

The modulation frequency necessary to compensate the actual Doppler effect of the moving system can be derived through a rigorous relativistic analysis. For this purpose, two coordinate systems are considered, the fixed frame S with coordinates $\{t, x, y, z\}$ and the moving frame S' with coordinates $\{t', x', y', z'\}$ as in Fig. 4(a).

The two sets are related to each other through a *Lorentz transformation* [29,30]: In the fixed frame S , the fields to the right of the reflector are $E_x = E_i e^{j(\omega_0 t + kz)} + E_r e^{j(\omega_1 t - k_1 z)}$, where $E_t = \rho E_i$ and ρ is the amplitude coefficient for the reflected mode as in Ref. [22], whereas in the moving frame S' the fields are as follows: $E'_x = E'_i e^{j(\omega'_0 t + k'z)} + \rho' E'_r e^{j(\omega'_1 t - k'_1 z)}$.

The frequencies and wave vectors in the fixed frame S are related to the ones in S' through

$$\begin{aligned} \omega_0 &= \omega'_0 \gamma (1 - \beta); & k &= \frac{\omega'_0}{c} \gamma (1 - \beta), \\ \omega_1 &= \omega'_0 \gamma (1 + \beta); & k_1 &= \frac{\omega'_0}{c} \gamma (1 + \beta), \end{aligned} \quad (3)$$

where $\beta = v_r/c$ and $\gamma = 1/\sqrt{1 - \beta^2}$ are the normalized velocity and the relativistic coefficient of the system, respectively.

In the moving frame S' , the incident field at frequency ω'_0 interacts with the modulated slab, and the reflected field will be at the frequency $\omega'_1 = \omega'_0 - \omega_m$. Therefore, it is possible to

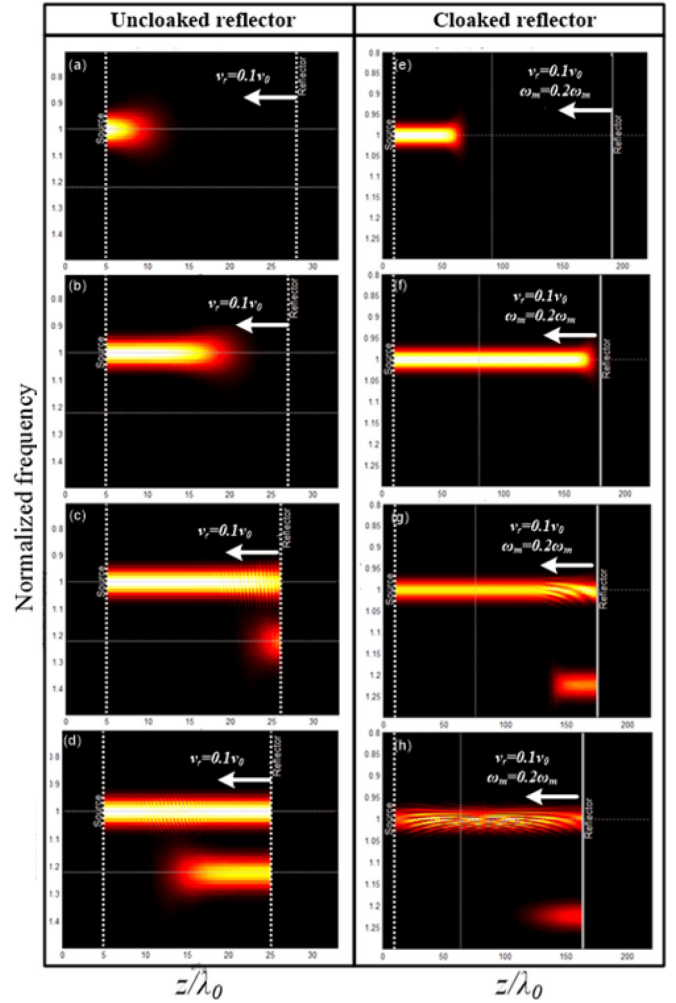


FIG. 5. FDTD simulations for a moving reflector (a)–(d) without and (e)–(h) with the Doppler cloak (the phantom line between source and reflector bounds the modulated region). The system is moving towards the source with a velocity $v_r = 0.1c$. In the case without the Doppler cloak, the reflected signal is shifted at a higher frequency $f = 1.22f_0$ with respect to the source frequency f_0 . On the other hand, in the case with the Doppler cloak, the reflected signal at $f = 1.22f_0$ interacts with the modulation wave of the permittivity profile that is co-directed with the reflected signal. The energy of the reflected signal is transferred back to the original frequency, leading to an observed zero-frequency shift and a zero apparent velocity for the system.

evaluate the reflected frequency ω_1 after taking into account the relativistic motion of the reflector as

$$\omega_1 = \omega_0 \frac{1 + \beta}{1 - \beta} - \omega_m \gamma (1 + \beta). \quad (4)$$

From Eq. (4), we can calculate the apparent velocity with which the system appears to be moving

$$\beta^{app} = \frac{2\beta\omega_0 - \omega_m\gamma^{-1}}{2\omega_0 - \omega_m\gamma^{-1}}. \quad (5)$$

This apparent velocity is a function of the actual velocity of the system and the modulation frequency and is plotted in Fig. 4(b) versus these two parameters. From this plot it is seen that the apparent velocity vanishes along the solid line, given by $\omega_m = 2\beta\gamma\omega_0$. This expression is found easily by taking β^{app} in Eq. (5) to be equal to zero. In Fig. 5, we show time-domain FDTD simulations for a system moving at relative velocity $\beta = 0.1$ with and without the one-dimensional Doppler cloak. The modulation frequency imparted to the cloak is the one providing apparent zero velocity according to Fig. 4(b). In the case without a Doppler cloak, the frequency of the reflected signal is $1.22f_0$ as expected from the Doppler effect. On the other hand, when the cloak is applied, the frequency of the reflected signal is the same as the one of the incident signal. The impinging signal passes through the cover and reaches the metallic reflector. There, it is reflected back at frequency $1.22f_0$ as expected, but the presence of the Doppler cloak allows transferring the energy again to the original frequency f_0 , fully compensating the Doppler effect.

In conclusion, we have introduced an approach to cancel the Doppler shift created by a moving object, realizing a cloak that can make a moving object appear stationary. The approach is based on covering the object with an active momentum-biased metamaterial layer that can produce an effective Doppler shift opposite to the actual one. The linear momentum-biased metamaterial implementing the Doppler cloak is a new kind of artificial dielectric, which has been proposed just a few years ago to realize magnetless nonreciprocal components [11–17]. The modulation of the permittivity profile can be achieved through different techniques, such as varactors at microwave frequencies or *p-i-n* junctions at optical frequencies, which load a transmission line locally modifying the effective permittivity function. In the case of the Doppler cloak, the matching between the free space and the modulated transmission line can be achieved using a transition layer. Here, we have demonstrated this idea in the case of a one-dimensional system, consisting of a perfect mirror and a spatiotemporally modulated slab that fully transforms the frequency of impinging waves. Our analysis shows that, for appropriately selected modulation frequency, the composite system looks stationary to an external observer, despite the fact that it is actually moving. Our results constitute a first step towards cloaking of moving objects and demonstrate the unique opportunities offered by active cloaks for overcoming fundamental limitations of their passive counterparts with relevant and direct implications for the minimization of electromagnetic and acoustic clutter caused by moving objects for radars and sonars.

This work was partially supported by the US Air Force Office of Scientific Research with Grant No. FA9550-13-1-0204 and the Simons Foundation.

-
- [1] J. B. Pendry, D. Schurig, and D. R. Smith, Controlling electromagnetic fields, *Science* **312**, 1780, (2006).
- [2] D. Schurig, J. J. Mock, B. J. Justice, S. A. Cummer, J. B. Pendry, A. F. Starr, and D. R. Smith, Metamaterial electromagnetic cloak at microwave frequencies, *Science* **314**, 977 (2006).
- [3] A. Alù and N. Engheta, Achieving transparency with plasmonic and metamaterial coatings, *Phys. Rev. E* **72**, 016623 (2005).
- [4] A. Alù, Mantle cloak: Invisibility induced by a surface, *Phys. Rev. B* **80**, 245115 (2009).
- [5] N. Engheta and R. W. Ziolkowski, *Metamaterials: Physics and Engineering Explorations* (Wiley, Hoboken, NJ, 2006).
- [6] F. Monticone and A. Alu, Do Cloaked Objects Really Scatter Less? *Phys. Rev. X* **3**, 041005 (2013).
- [7] J. C. Halimeh, R. T. Thompson, and M. Wegener, Invisibility cloaks in relativistic motion, *Phys. Rev. A* **93**, 013850 (2016).
- [8] E. N. da C. Andrade, *Doppler and the Doppler Effect* (Endeavour, London, 1959), Vol. 18, pp. 14–19.
- [9] P.-Y. Chen and A. Alù, Mantle cloaking using thin patterned metasurfaces, *Phys. Rev. B* **84**, 205110 (2011).
- [10] Z. Yu and S. Fan, Complete optical isolation created by indirect interband photonic transitions, *Nat. Photonics* **3**, 91 (2009).
- [11] H. Lira, Z. Yu, S. Fan, and M. Lipson, Electrically Driven Non Reciprocity Induced by Inter-band Photonic Transition on a Silicon Chip, *Phys. Rev. Lett.* **109**, 033901 (2012).
- [12] D. L. Sounas, C. Caloz, and A. Alù, Giant non-reciprocity at the subwavelength scale using angular momentum-biased metamaterials, *Nat. Commun.* **4**, 2407 (2013).
- [13] D. L. Sounas and A. Alù, Angular-momentum-biased nanorings to realize magnetic-free integrated optical isolation, *ACS Photonics* **1**, 198 (2014).
- [14] R. Fleury, D. L. Sounas, C. F. Sieck, M. R. Haberman, and A. Alù, Sound isolation and giant linear nonreciprocity in a compact acoustic circulator, *Science* **343**, 516 (2014).
- [15] N. A. Estep, D. L. Sounas, J. Soric, and A. Alù, Magnetic-free non-reciprocity and isolation based on parametrically modulated coupled-resonator loops, *Nat. Phys.* **10**, 923 (2014).
- [16] D. Ramaccia, D. L. Sounas, A. Alù, F. Bilotti, and A. Toscano, Non-reciprocal filtering horn antennas using angular momentum-biased metamaterial inclusions, *IEEE Trans. Antennas Propag.* **63**, 5593 (2015).
- [17] Y. Hadad, D. L. Sounas, and A. Alù, Space-Time Gradient Metasurfaces, *Phys. Rev. B* **92**, 100304(R) (2015).
- [18] Q. Jiang, *Network Radar Countermeasure Systems* (Springer, Berlin/Heidelberg, 2015).
- [19] P.-Y. Chen, C. Argyropoulos, and A. Alù, Broadening the Cloaking Bandwidth with Non-Foster Metasurfaces, *Phys. Rev. Lett.* **111**, 233001 (2013).

- [20] M. Selvanayagam and G. V. Eleftheriades, Experimental Demonstration of Active Electromagnetic Cloaking, *Phys. Rev. X* **3**, 041011 (2013).
- [21] D. L. Sounas, R. Fleury, and A. Alù, Unidirectional Cloaking Based on Metasurfaces with Balanced Loss and Gain, *Phys. Rev. Appl.* **4**, 014005 (2015).
- [22] D.-W. Wang, H.-T. Zhou, M.-J. Guo, J.-X. Zhang, J. Evers, and S.-Y. Zhu, Optical Diode Made from a Moving Photonic Crystal, *Phys. Rev. Lett.* **110**, 093901 (2013).
- [23] J. N. Winn, S. Fan, J. D. Joannopoulos, and E. P. Ippen, Interband transitions in photonic crystals, *Phys. Rev. B* **59**, 1551 (1998).
- [24] See Supplemental Material at <http://link.aps.org/supplemental/10.1103/PhysRevB.95.075113> for coupled-mode analysis of the spatiotemporally modulated slab.
- [25] A. Yariv, *Optical Electronics*, 4th ed. (Harcourt Brace College, Fort Worth, TX, 1991).
- [26] See Supplemental Material at <http://link.aps.org/supplemental/10.1103/PhysRevB.95.075113> for angular and frequency bandwidths of the Doppler cloak.
- [27] See Supplemental Material at <http://link.aps.org/supplemental/10.1103/PhysRevB.95.075113> for FDTD: co- and contradirected propagation in a linear momentum-biased MTM slab.
- [28] See Supplemental Material at <http://link.aps.org/supplemental/10.1103/PhysRevB.95.075113> for a parallel-plate linear momentum-biased metamaterial medium.
- [29] S. J. Orfanidis, *Electromagnetic waves and antennas*, free online book available at www.ece.rutgers.edu/~orfanidi/ewa (2008).
- [30] C. Yeh and K. F. Casey, Reflection and transmission of electromagnetic waves by a moving dielectric slab, *Phys. Rev.* **144**, 665 (1966).